



## On the flexural properties of multiscale nanosilica/E-glass/epoxy anisogrid-stiffened composite panels

Hamed Khosravi<sup>a,b</sup> and Reza Eslami-Farsani<sup>a,\*</sup>

<sup>a</sup> Faculty of Materials Science and Engineering, K. N. Toosi University of Technology, Tehran, Iran.

<sup>b</sup> Department of Materials Engineering, Faculty of Engineering, University of Sistan and Baluchestan, Zahedan, Iran

---

**Article info:**

Received: 08/04/2016

Accepted: 28/01/2017

Online: 15/07/2017

---

**Keywords:**

Anisogrid-stiffened composite structure, Multiscale composite, Silica nanoparticle, Surface modification, 3-point bending response, Energy absorption.

---

**Abstract**

In the present study, multiscale nanosilica/E-glass/epoxy anisogrid composite panels were investigated for flexural properties as a function of nanosilica loading in the matrix (0, 1, 3 and 5 wt. %). The surface of the silica nanoparticles was firstly modified with 3-glycidoxypropyltrimethoxysilane. The Fourier transform infrared spectroscopy revealed that the organic functional groups of the silane were successfully chemically grafted on the surface of the nanoparticles. It was illustrated that flexural properties of the composite panel loaded from the skin side can be significantly enhanced by incorporating silica nanoparticles. From the 3-point flexural test, it was found that using of 3 wt. % nanosilica was the most effective in increasing the load bearing capacity and energy absorption value, while the specimen containing 5 wt. % nanosilica demonstrated the highest flexural stiffness. The results obtained for the anisogrid panels loaded from the skin side showed that these structures displayed excellent damage resistance which is represented by their energy absorption capability. Moreover, a significant portion of energy absorbed after the primary failure at the peak load. Finally, the results correlated well with the observation of field emission scanning electron microscopy micrographs where the nanocomposite panels exhibited higher degree of fiber-matrix interfacial strength and also enhanced matrix characteristics, imparted by the incorporation of surface modified silica nanoparticles.

---

### 1. Introduction

Grid-stiffened composite (GSC) structures are a class of composite materials in which a grid of unidirectional composite ribs (stiffeners) is supported by a shell structure namely skin. These structures derive their strength from their

ribs [1]. The main advantages of using the grid structures are their high strength and stiffness to weight ratios, high energy absorption, and excellent damage tolerance. Due to the advantages mentioned above, the GSC structures find many applications in various industries such as aerospace, airplane, automotive, and ship building [2]. The loading

---

\*Corresponding author  
email address: [eslami@kntu.ac.ir](mailto:eslami@kntu.ac.ir)

capacity and weight efficiency of the grid composites are higher than that of the traditional bending dominated cellular materials such as foams and honeycombs. A comprehensive review paper about the history of the GSC structures, the fabrication methods, the founding studies, and also the analysis of design approaches is presented by Vasiliev et al. [3]. A GSC structure can be failed in various failure modes including fiber breakage, cracking and fracture of the matrix, delamination, shear degradation modes, rib-skin debonding or a combination of the above. The geometric parameters such as rib cross-section, skin thickness, rib angle, etc. have profound effects on the final performance of these composite structures. For this reason, some experimental and theoretical studies have been conducted by several authors and reported in the literature [4-10].

Fan et al. [4] showed that the imperfections of lattice materials, such as the waviness of the struts, non-circular cross sections and cantilever ribs, greatly influenced their performance. Akhl et al. [5] studied the optimization of the static and dynamic characteristics of plates with isogrid stiffeners. The static characteristics were optimized by maximizing the critical buckling loads of the plate, while the dynamic characteristics were optimized through maximizing multiple natural frequencies. Gibson [6] conducted an analytical/experimental study of the energy absorption characteristics of grid-stiffened composite structures under transverse loading. The results showed that these types of structures had excellent energy absorption characteristics, and most of the absorbed energy occurred beyond initial failure. In the work of Kim [7], the rib buckling was found to be the critical failure mode for the isogrid plate under the compressive loads. The isogrid plate was demonstrated to be tolerant to structural damage due to the multiplicity of load paths. Jadhav et al. [8] assessed the energy absorption and damage evaluation of grid stiffened composite panels under transverse loading. Results of this work showed that loading the panels on rib side resulted in greater specific energy absorption along with larger displacements compared to

skin side loading which was more abrupt. Also, the optimization of geometry to maximize the specific energy absorption of E-glass/polypropylene isogrid composite panels under transverse quasi-static and dynamic impact loading using finite element analysis was investigated by the same authors [9]. Parametric studies of varying the rib width and thickness, the center-to-center distance between rib joints and skin thickness to maximize specific energy absorption were conducted. Wodesenbet et al. [10] reported the results of optimization for buckling loads of grid stiffened composite panels. An improved smeared method was developed to model the buckling problem of an isogrid stiffened composite cylinder.

It has been reported in the literature that the addition of nanoparticles can effectively enhance the mechanical properties of the fibrous composites. Such type of composites containing both of the micro and nano reinforcements is called multiscale composite [11, 12]. Adding nanoparticles into fiber-reinforced polymers creates new composite materials which have new favorable properties for different applications.

The nanosilica in the multiscale hybrid composites not only can grow directly on the fiber but also dispersed in the matrix. Uddin et al. [13] used a modified vacuum assisted resin transfer molding (VARTM) process to fabricate SiO<sub>2</sub>/unidirectional glass fiber/epoxy composites and reported that inclusion of nanosilica particles increased longitudinal compressive and tensile strengths of specimens compared with conventional unidirectional glass fiber/epoxy composites. Chira et al. [14] reported that tensile strength of alkali resistant glass fiber reinforced epoxy composites increased up to 68% by adding only 2 wt. % of silica nanoparticles. Rostamiyan et al. [15] reported that with the addition of 3.5 wt. % silica nanoparticles, the flexural strength of glass fiber reinforced epoxy composite was increased 50% in comparison with samples without silica nanoparticles. Jacob et al. [16] investigated the reinforcing effect of nano-SiO<sub>2</sub> on polypropylene-nylon fibrous composites. They reported composite specimens with 1 wt.

% nano-SiO<sub>2</sub> and 30 wt. % nylon fiber showed higher tensile strength, tensile modulus, flexural strength and flexural modulus. Gong et al. [17] reported that tensile strength of glass fiber reinforced epoxy composites was increased up to 22% by adding only 15 wt. % silica nanoparticles. In the work of Gong et al. [17], epoxy modified with nanosilica as new “matrix” for the composites has been shown to be a possibility to enhance the interfacial properties between fiber bundle and “matrix”. The interfacial strength between fiber bundle and the “matrix” was enhanced by ~58.3 %. The outcomes of the research work conducted by Panse et al. [18] are: (1) compressive strength of hybrid glass or carbon fiber/epoxy composites showed more than 30-35% increase with nanosilica at a concentration of as low as 0.2 wt. %, and (2) tensile and compressive properties of hybrid composites in transverse direction to the reinforcement remained unaffected.

The aim of this research is to study the reinforcing effect of nanosilica particles on the flexural properties of epoxy/E-glass anisogrid-stiffened composite panels under three-point bending test. The influence of adding nanosilica particles at different weight percentages of the epoxy matrix (0, 1, 3 and 5) on the flexural properties of composite panels investigated. Based on the fracture surface analysis, the possible mechanisms were proposed and discussed.

## 2. Experimental

### 2.1. Materials

The matrix used in composites for the current study was an ML-506 epoxy resin based on epoxy bisphenol F with hardener HA-11, supplied by Mokarrar Engineering Materials Co, Iran. The resin- hardener ratio was 100:15 by weight, as recommended by the manufacturer. This resin system was chosen because of its low viscosity (1450 centipoise) and long gel time (60 min) at 25°C. Also, the mixed system density was 1.1 g/cm<sup>3</sup>. The tensile and flexural strengths of employed resin were 761 and 960 kgf/cm<sup>2</sup>, respectively.

Unidirectional E-glass fiber (density: 2.58 g/cm<sup>3</sup>, average diameter: 12 μm) and 2 dimensional plain weave E-glass fabric (surface density: 400 g/m<sup>2</sup>), both supplied by LINTEX International Co., Ltd, China, were used as fibrous reinforcements. The silica nanoparticles as filler part were purchased from US Research Nanomaterials, Inc, USA. Figure 1 illustrates FE-SEM, HITACHI S-4160, 25 kV) image of as-received silica nanoparticles having an average size of 65 nm and specific surface area of 380 m<sup>2</sup>/g. 3-Glycidoxypopyltrimethoxysilane (3-GPTS), with the molecular formula of C<sub>9</sub>H<sub>20</sub>O<sub>5</sub>Si, as a silane coupling agent was provided by Merck Chemical Co, Germany. This compound was selected because of its epoxide groups which can easily react with the epoxy matrix in the presence of amine hardener.

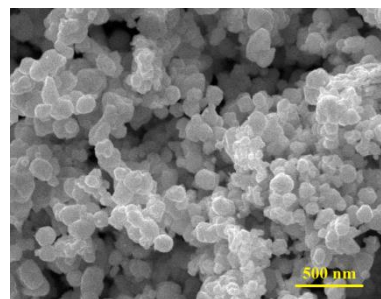


**Fig. 1.** FE-SEM image of as-received silica nanoparticles.

### 2.2. Surface treatment of nanosilica

2.0 g nanosilica and 2.0 g 3-GPTS were added to 100 ml of 95% ethanol solution. Afterwards, this mixture was stirred for 10 min using a probe sonicator and then refluxed at 70°C for 12 h under constant low-speed magnetic stirring for 100 rpm. The pH value of the mixture was adjusted to be about 4-5, with the aid of 37% concentrated HCl. In the final stage, the nanosilica particles were centrifuged, and the precipitates were washed twice with ethanol (50 mL) for 3 h to remove the excess silane coupling agent absorbed on the silica surfaces [19].

### 2.3. Preparation of silicone mold

In the present study, composite panels with an anisogrid lattice patterned reinforcements were fabricated. Silicone molds were used to fabricate the grid specimens. The main reasons of selecting silicone for making molds were its rubber state and bearing high elastic strains, which facilitate the removal of the specimen from the mold. The silicone compound used in this research consisted of RTV-3325 and 6H components which were mixed in 100:4 ratio by weight. The molds were obtained by pouring liquid silicone mixture over a pre-fabricated polyvinyl chloride (PVC) model (Fig. 2(a)) and then holding at room temperature for about 6 h to make it cure. The silicone mold is shown in Fig. 2(b).

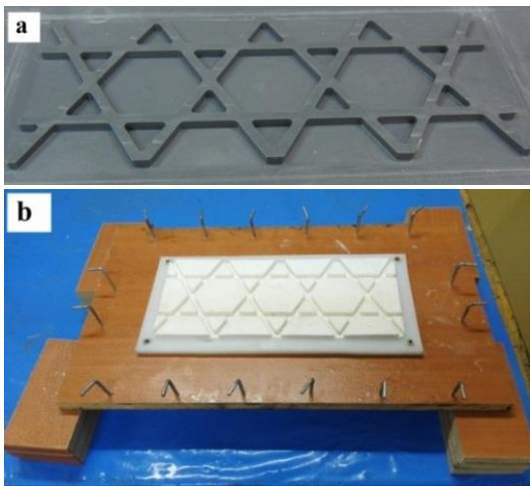


**Fig. 2.** (a) PVC model and (b) silicone mold.

### 2.4. Fabrication of specimens

For the nanocomposite fabrication, a mixture of weighed amount of surface modified silica nanoparticles with epoxy resin was firstly stirred by a high-speed mixer (SDS-11D, Fintek Co., Korea) at a rotation speed of 2000 rpm for 20 min. The mixture was further ultrasonically homogenized using a probe of 14-mm tip diameter; at 120 W and 30% duty cycle (Ultrasonic Homogenizer 400 W, 24 kHz, FAPAN Co., Ltd., Iran) for 90 min. Afterwards, the mixture after cooling to room temperature was kept under vacuum for 20 min to facilitate the release of any entrapped air. The resultant

mixture was then employed for fabricating the multiscale composite panels. Three different nanosilica loadings of 1, 3 and 5 wt. % in the epoxy resin were prepared.

The fabrication of the anisogrid composite panels was performed using a methodology indicated in Fig. 3. Unidirectional E-glass fiber rovings were impregnated with the matrix resin and then laid up into grooves of silicone mold layer by layer to form the ribs of grid structure. In the next step, laying up the skin using 4 layers of E-glass woven fabrics was carried out. The skin thickness of all the specimens was 1.8 mm. After completion of the manufacturing process, curing process of resin was performed within 3 h. In order to achieve maximum strength and ultimate curing, the specimens were left at room temperature for 7 days. The fabricated specimens are shown in Fig. 4. The cross-section area of all ribs was a quadrangle with the area of  $6 \times 6 \text{ mm}^2$ . The specimens were characterized by length of a 300mm and width of 125mm. For the purpose of comparison, an anisogrid panel without nanosilica incorporation was also fabricated. The total volume fraction of glass fibers was 44% and 48% in ribs and skin parts, respectively.

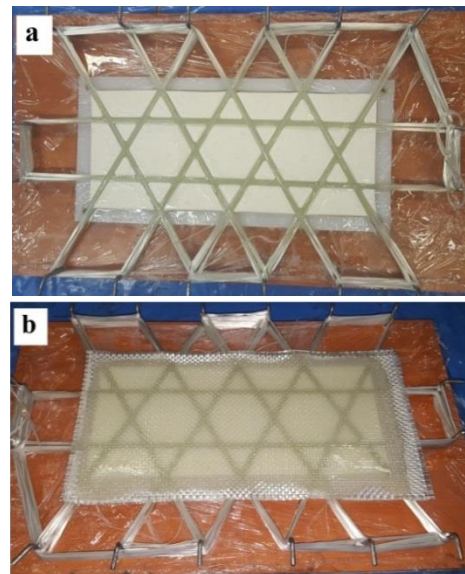


**Fig. 3.** The method employed for fabricating the AGS panels, (a) rib formation and (b) skin fabrication.

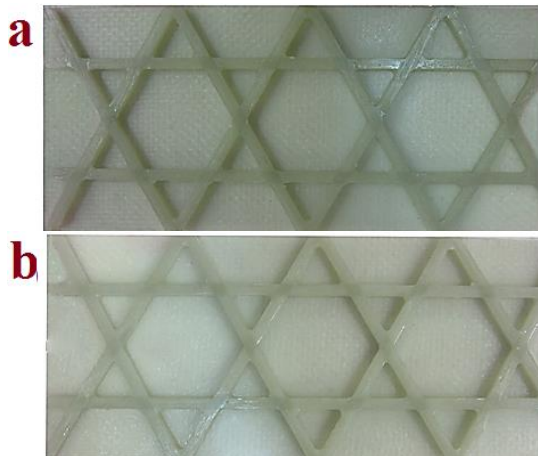


**Fig. 4.** Anisogrid GSC panels, (a) without nanosilica addition and (b) containing nanosilica.

2.5. 3-point flexural test

The flexural properties of the anisogrid panels were obtained according to the ASTM: D7264-07. A Hounsfield: H25K apparatus was used to run the 3-point flexural test. The specimens were loaded to a displacement of 80 mm at a cross-head speed of 5 mm/min. Three specimens were used for each measurement. The representation of the setup used for the flexural test is shown in Fig. 5. All the panels were loaded from the skin side, while the span length was kept to 250 mm. During the loading, the flexural load as a function of axial displacement was recorded for each specimen.

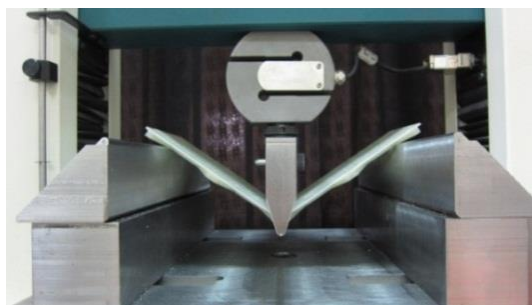


**Fig. 5.** Experimental setup for three-point bending test.

2.6. Characterization

Fourier transform infrared (FT-IR) spectra of the as-received and 3-GPTS modified nanosilica were recorded on a JASCO FTIR

spectrometer (FTIR-460 plus) with KBr pellets at a resolution of 4 cm<sup>-1</sup> to observe the functional groups on the nanosilica surface. The fracture surface of the specimens was analyzed using the FE-SEM after the test.

3. Results and discussion

3.1. FT-IR results

Figure 6 gives the FTIR spectra of as-received nanosilica, 3-GPTS coupling agent and silane-modified nanosilica (3-GPTS/nanosilica). On the spectrum of the unmodified nanosilica, appearance of the peaks at 3397 cm<sup>-1</sup> is indicative of the presence of hydroxyl groups (O-H) on the surface of nanosilica, while the observed peaks at 1628, 1108, 817 and 469 cm<sup>-1</sup> are corroborated to be Si-O-Si stretching vibrations [19,20].

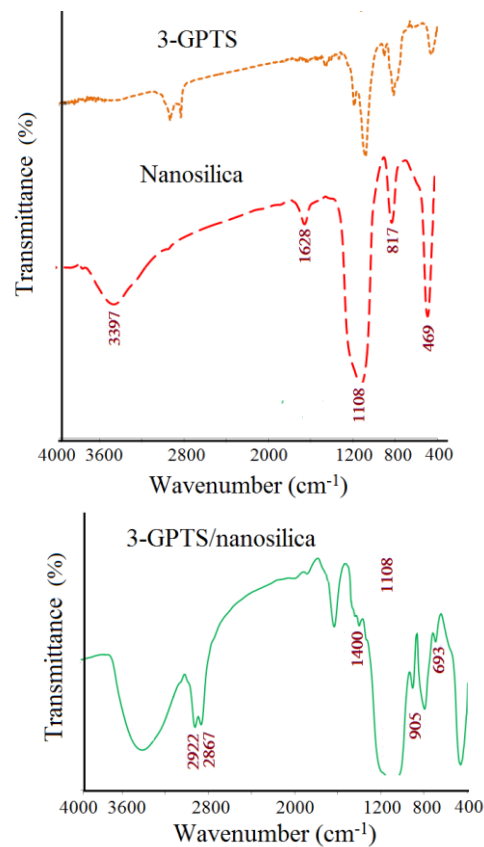


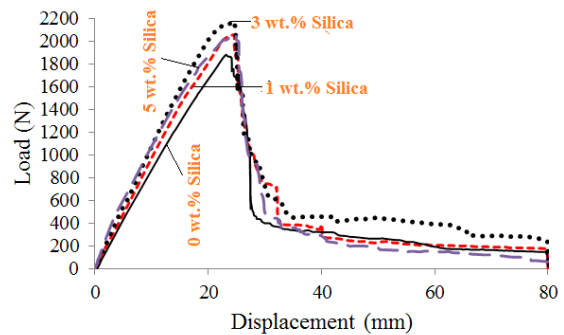
**Fig. 6.** The FT-IR spectra of as-received nanosilica, 3-GPTS coupling agent and silane-modified nanosilica.

The FTIR spectrum of 3-GPTS/nanosilica illustrates additional peaks at 1400, 905 and 693  $\text{cm}^{-1}$ , which are absent in the FT-IR spectrum of untreated nanosilica particles. These peaks are related to the vibration of epoxide groups grafted on the nanosilica surface [20, 21]. The peaks at 2,928 and 2,880  $\text{cm}^{-1}$  correspond to the asymmetrical and symmetrical stretching of  $\text{CH}_3$  and  $\text{CH}_2$  groups, respectively [11]. When the 3-GPTS/nanosilica particles are incorporated in the epoxy resin and the amine hardener is added, the epoxide end of the 3-GPTS involves in the crosslinking with the epoxy and as a result, a strong covalent bond is formed between the epoxy and nanosilica [19].

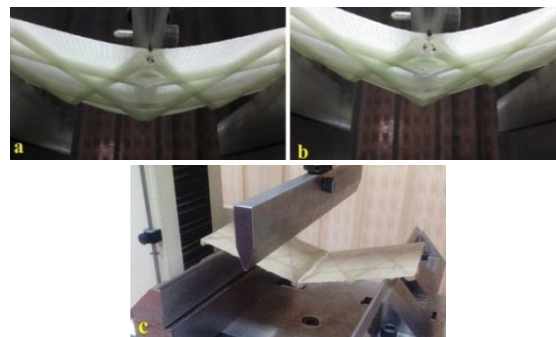
### 3.2. The results of flexural test

Figure 7 illustrates the flexural load-displacement curves for the multiscale E-glass/epoxy/nanosilica GSC panels containing various amounts of 3-GPTS/nanosilica. The load-displacement responses for all GSC panels are shown a similar trend. Note that, the panels were loaded from the skin side up to a displacement of 80 mm. Initially, all the curves show a linear increase in load, however with different slopes. Then, the slope of load increase is declined until reaching the peak load. Interestingly, a considerable portion of energy absorption is observed after the primary failure at peak load. When the panels are loaded on the skin side, various failure modes are observable, as indicated in Fig. 8. In an anisogrid panel, fiber breakage and fiber microbuckling are two damage mechanisms occurring under transverse loading from the skin side. Under flexural loading, the longitudinal ribs of the panel along with skin sustain the maximum applied load. The flexural properties of the anisogrid panels containing various amounts of nanosilica were extracted from Fig. 7. The obtained data are illustrated in Figs. 8 and 9. It can be seen in Fig. 8(a) that the flexural stiffness enhances with an increase in the nanosilica loading. Flexural stiffness is defined as the slope of a linear portion of the load-displacement curve. At 5 wt. % 3-GPTS/nanosilica, the anisogrid panel illustrates a 23% enhancement in the flexural stiffness. The improvement in the flexural

stiffness is expected due to the higher modulus of silica compared to the epoxy matrix. Also, the good interfacial interactions between the silane modified silica nanoparticles and the epoxy matrix restrict the mobility of polymer chains under loading and allow shear deformation and stress to transfer from the matrix to the nanosilica particles.



**Fig. 7.** Flexural load-displacement curves for the E-glass/epoxy/nanosilica anisogrid panels at different nanosilica contents.



**Fig. 8.** Fracture modes observed during flexural loading of a neat GSC panel at a displacements of (a) 23 mm, (b) 32 mm, and (c) 80 mm.

The obtained load bearing capacity of neat anisogrid E-glass/epoxy composite, indicated by peak load in the curve, is 1882 N. By adding 3-GPTS/nanosilica, the load bearing capacity of the specimens is firstly increased and afterwards declined, as indicated in Fig. 8(b). At 3 wt. % nanosilica, the load bearing capacity is enhanced by 15%. This may have two reasons: First, the interfacial characteristics of the E-glass fibers and matrix should be considered. It has been generally accepted that one of the main parameters affecting the mechanical properties of fibrous composites is the fiber-matrix interphase [22].

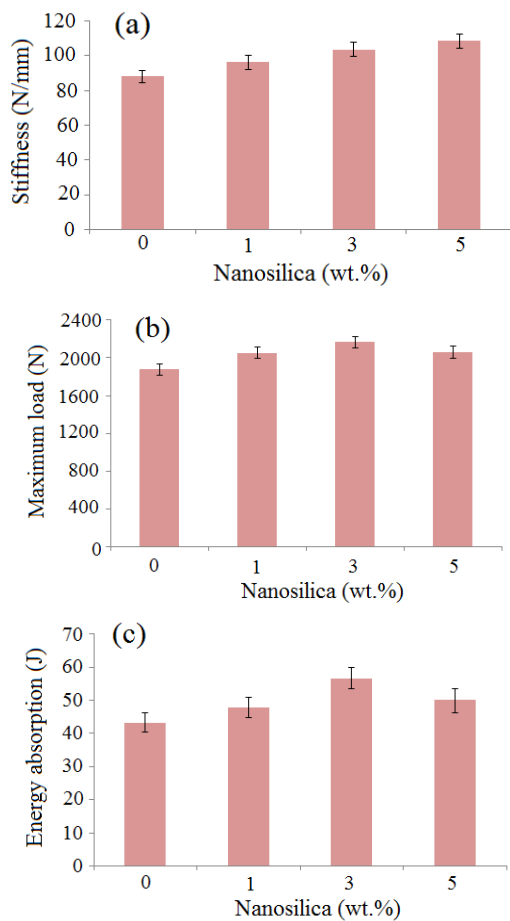


**Fig. 9.** Variation of (a) stiffness, (b) maximum load, and (c) energy absorption versus nanosilica loading.

The mismatch of coefficient of thermal expansion (CTE) between the E-glass fiber and matrix could result in high residual stresses in the interface zone because of matrix shrinkage during the curing process. The incorporation of nanosilica decreases the CTE of the matrix and reduces the residual stresses in the interface [17]. This can lead to suppressing the fiber/matrix debonding. The second reason is attributed to the reinforcing effect of 3-GPTS/nanosilica in the matrix part. In a fiber reinforced composite, there are two important zones of stress concentration, fibers (especially fiber skin) and fiber-matrix interphase [23]. When the matrix is reinforced through the nanosilica addition, the stress level in these regions is decreased. However, at 5 wt. % nanosilica loading, the load bearing capacity of the specimen decreases compared to that

specimen containing 3 wt. % nanosilica. This can be explained as, at higher nanosilica loading, the formation of a continuous matrix network is prevented and thus the adhesion between the matrix and fibers is declined. Also, at high loadings of a nanoparticle, the epoxy resin viscosity significantly increases affecting its curing and cross-linking density. This observation is in line with the literature [24]. It can be observed from histograms in Fig. 9 that there is a significant improvement in the energy absorption by incorporating 3-GPTS/nanosilica in the composites. The addition of nanosilica in the epoxy matrix assists in the postponement of crack initiation or hinders the crack propagation through the deflection mechanism.

In fibrous composites, matrix cracking and fiber-matrix debonding are main mechanisms occurring during loading. Because elastic modulus of nanosilica compared to epoxy is high, so stress gradient in the vicinity of fillers can lead to the creation of high-stress concentration in these regions and formation of micro-cracks. Nanosilica can alter the crack deflection as a result of stress redistribution in the matrix and lead to increase the crack propagation path. Increasing the weight percentage of nanosilica from 3 to 5 can result in more agglomerate formation. It seems that the presence of agglomerations can be the main reason for decreasing the energy absorption of the composites at higher silica contents.

### 3.3. Microstructural observations

The findings from FE-SEM observations support the quantitative results of the mechanical testing. Fig. 10 depicts the fractographs of the central rib for the neat and multiscale ASC panels. On comparing Figs. 10(a) and 10(b), it can be seen that the interfacial bonding in the multiscale specimen containing 3 wt. % of nanosilica particles is superior to that in the neat specimen free from the nanosilica particles. Regarding Fig. 10(a) which is related to the neat central rib, the surface morphology of the fibers is observed to be very clean and smooth. This indicates that the interfacial de-bonding is the main failure mechanism for this specimen [25]. On the

contrary, as it can be clearly seen in Fig. 10(b), there is a very good adhesion between the components for the multiscale specimen. Such finding indicates that the matrix cracking is the primary failure mechanism for this specimen [25]. Consequently, enhanced interfacial bonding fosters the stress transfer and facilitates the composite to endure higher loads without any plastically deforming [26]. Fig. 10(c) depicts that the neat specimen contains the matrix regions that are even, representing the brittle fracture. For this specimen, shear stress is transmitted slowly from one layer to another and there exists a little difference between the layers. The fracture surface of the nanosilica/epoxy nanocomposite matrix (Fig. 10d), however, shows a substantial increase in the surface roughness, which indicates the reinforcement by the nanosilica in the epoxy matrix. This phenomenon is due to the crack deflection mechanism.

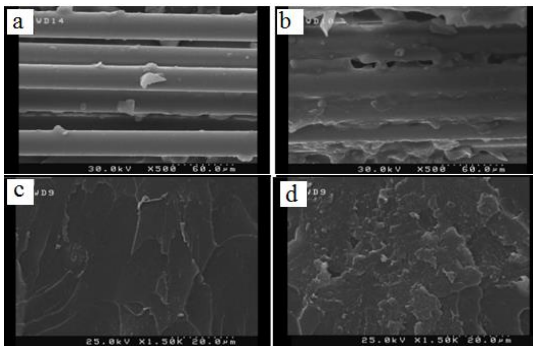


**Fig. 10.** FE-SEM micrographs of fracture surfaces of central rib with epoxy resin matrix: (a, c) unmodified and (b, d) with 3 wt. % nanosilica.

**4. Conclusions**

The multiscale anisogrid E-glass/epoxy/nanosilica composite panels containing different contents of surface-modified nanosilica were fabricated in this work. The 3-point flexural properties of the panels were evaluated. The results of this investigation can be summarized as follows:

1) Nanosilica particles were successfully surface-modified using 3-GPTS. The FT-IR analyst confirmed the presence of 3-GPTS in the structure of nanosilica after modification stage.

2) Matrix reinforcing with surface-modified nanosilica was found to significantly enhance the flexural response of GSC panels.

3) Adding the nanosilica to the matrix of the composites resulted in continues increasing of their flexural stiffness. The load bearing capacity and energy absorption of the specimens was firstly increased and then declined by increasing the nanosilica loadings. At 3 wt. % nanosilica loading, the highest load bearing capacity, and energy absorption were obtained.

4) GSC panels showed high damage tolerance. In these structures, a considerable fraction of energy absorption was observed after the primary failure occurring at the peak load point.

**References**

[1] V. V. Vasiliev, V. A. Barynin, and A. F. Razin, "Anisogrid composite lattice structures-Development and aerospace applications", *Composite Structures*, Vol. 94, No. 3, pp. 1117-1127, (2012).

[2] V. V. Vasiliev, and A. F. Razin, "Anisogrid composite lattice structures for spacecraft and aircraft applications", *Composite Structures*, Vol. 76, No. 1-2, pp. 182-189, (2006).

[3] V. V. Vasiliev, V. A. Barynin, A. F. Rasin, S. A. Petrokovskii, and V. I. Khalimanovich, "Anisogrid composite lattice structures-development and space applications", *Composite structures*, Vol. 3, pp. 38-50, (2009).

[4] H. Fan, F. Jin, and D. Fang, "Characterization of edge effects of composite lattice structures", *Composites Science and Technology*, Vol. 69, No. 11-12, pp. 1896-1903, (2009).

[5] W. Akl, A. El-Sabbagh, and A. Baz, "Optimization of the static and dynamic characteristics of plates with isogrid stiffeners", *Finite Elements in Analysis and Design*, Vol. 44, No. 8, pp. 513-523, (2008).

[6] F. R. Gibson, "Energy absorption in composite grid structures", *Advanced Composite Materials*, Vol. 14, No. 2, pp. 113-119, (2005).



- [7] T. D. Kim, "Fabrication and testing of thin composite isogrid stiffened panel", *Composite Structures*, Vol. 49, No. 1, pp. 21-25, (2000).
- [8] P. Jadhav, and P. R. Mantena, "Parametric optimization of grid-stiffened composite panels for maximizing their performance under transverse loading", *Composite Structures*, Vol. 77, No. 3, pp. 353-363, (2007).
- [9] P. Jadhav, and P. R. Mantena, "Impact response and damage evaluation of grid stiffened composite panels", *SEM Annual Conference and Exposition on Experimental and Applied Mechanics*, USA, (2005).
- [10] E. Wodesenbet, S. Kidane, and S. S. Pang, "Optimization for buckling loads of grid stiffened composite panels", *Composite Structures*, Vol. 60, No. 2, pp. 159-169, (2003).
- [11] H. Khosravi, and R. Eslami-Farsani, "On the mechanical characterizations of unidirectional basalt fiber/epoxy laminated composites with 3-glycidoxypropyltrimethoxysilane functionalized multi-walled carbon nanotubes-enhanced matrix", *Journal of Reinforced Plastics and Composites*, Vol. 35, No. 5, pp. 421-434, (2016).
- [12] M. M. Shokrieh, A. Saeedi, and M. Chitsazzadeh, "Evaluating the effects of multi-walled carbon nanotubes on the mechanical properties of chopped strand mat/polyester composites", *Materials and Design*, Vol. 56, pp. 274-279, (2014).
- [13] M. F. Uddin, and C. T. Sun, "Strength of unidirectional glass/epoxy composite with silica nanoparticle-enhanced matrix", *Composites Science and Technology*, Vol. 68, No. 7-8, pp. 1637-1643, (2008).
- [14] A. Chira, A. Kumar, T.V Iach, L. Laiblova, A. S. Skapin, and P. Hajek, "Property improvements of alkali resistant glass fibers/epoxy composite with nanosilica for textile reinforced concrete applications", *Materials and Design*, Vol. 89, pp. 146-155, (2016).
- [15] Y. Rostamiyana, A. Fereidoonb, M. Rezaeiashtiyanic, A. H. Mashhadzadeh, and A. Salmankhani, "Experimental and optimizing flexural strength of epoxy-based nanocomposite: Effect of using nano silica and nano clay by using response surface design methodology", *Materials and Design*, Vol. 69, pp. 96-104, (2015).
- [16] S. Jacob, K. K. Suma, J. M. Mendez, and K. E. George, "Reinforcing effect of nanosilica on polypropylene-nylon fiber composite", *Materials Science and Engineering: B*, Vol. 168, No. 1-3, pp. 245-249, (2010).
- [17] L. X. Gong, L. L. Hu, J. Zang, Y. B. Pei, L. Zhao, and L. C. Tang, "Improved interfacial properties between glass fibers and tetra-functional epoxy resins modified with silica nanoparticles", *Fibers and Polymers*, Vol.16, No. 9, pp. 2056-2065, (2015).
- [18] P. Panse, A. Anand, V. Murkute, A. Ecka, R. Harshe, and M. Joshi, "Mechanical properties of hybrid structural composites reinforced with nanosilica", *Polymer Composites*, Vol. 37, No.4, pp. 1216-1222, (2016).
- [19] H. Khosravi, and R. Eslami-Farsani, "An experimental investigation into the effect of surface-modified silica nanoparticles on the mechanical behavior of E-glass/epoxy grid composite panels under transverse loading", *Journal of Science and Technology of Composites*, Vol. 3, No. 1, pp. 11-20, 2016 (In Persian).
- [20] Y. YE, X. Zeng, H. Qiangli, P. Chen, and C. Ye, "Synthesis and characterization of nanosilica/ polyacrylate composite emulsions by sol-gel method and in-situ emulsion polymerization", *Journal of Macromolecular Science Part A*, Vol. 48, No. 1, pp. 42-46, (2011).
- [21] D. K. Shukla, S. V. Kasisomayajula, and V. Parameswaran, "Epoxy composites using functionalized alumina platelets as reinforcements", *Composite Science and Technology*, Vol. 68, No. 14, pp. 3055-3063, (2008).

- [22] N. A. Siddiqui, S. U. Khan and J. K. Kim, "Experimental torsional shear properties of carbon fiber reinforced epoxy composites containing carbon nanotubes", *Composite Structures*, Vol. 104, pp. 230-238, (2013).
- [23] S. Houshyar, A. Shanks, and A. Hodzic, "Modelling of polypropylene fiber-matrix composites using finite element analysis", *eXPRESS Polymer Letters*, Vol. 3, No. 1, pp. 2-12, (2009).
- [24] A. Mirzapour, M. H. Asadollahi, S. Baghshaei, and M. Akbari, "Effect of nanosilica on the microstructure, thermal properties and bending strength of nanosilica modified carbon fiber/phenolic nanocomposite", *Composites: Part A*, Vol. 63, pp. 159-167, (2014).
- [25] R. Eslami-Farsani, S. M. R. Khalili, Z. Hedayatnasab, and N. Soleimani, "Influence of thermal conditions on the tensile properties of basalt fiber reinforced polypropylene-clay nanocomposites", *Materials and Design*, Vol. 53, pp. 540-549, (2014).
- [26] D. R. Bortz, C. Merino, and I. Martin-Gullon, "Mechanical characterization of hierarchical carbon fiber/nanofibercomposite laminates", *Composites: Part A*, Vol. 42, No. 11, pp. 1584-1591, (2011).

### How to cite this paper:

Hamed Khosravi and Reza Eslami-Farsani, "On the flexural properties of multiscale nanosilica/E-glass/epoxy anisogrid-stiffened composite panels", *Journal of Computational and Applied Research in Mechanical Engineering*, Vol. 7. No. 1, pp. 99-108

**DOI:** 10.22061/JCARME.2017.638

**URL:** [http://jcarme.srttu.edu/article\\_638.html](http://jcarme.srttu.edu/article_638.html)

